

Thermally Induced Grafting Reactions of Ethylene Glycol and Glycerol Intercalates of Kaolinite

Marián Janek,^{*,†,‡} Katja Emmerich,^{§,||} Stefan Heissler,[§] and Rolf Nüesch^{§,||}

Department of Physical and Theoretical Chemistry, Faculty of Natural Sciences, Comenius University, Mlynská dolina CH1, SK-84215 Bratislava, Slovakia, and Institute of Inorganic Chemistry, Slovak Academy of Sciences, Dúbravská cesta 9, SK-84536 Bratislava, Slovakia, Institute for Technical Chemistry, Water- and Geotechnology, Research Centre Karlsruhe GmbH, P.O. Box 3640, D-76021 Karlsruhe, Germany, and Soil Moisture Group, University Karlsruhe, Kaiserstrasse 12, D-76131 Karlsruhe, Germany

Received June 26, 2006. Revised Manuscript Received November 28, 2006

Inorganic-organic layered hybrid materials based on kaolinite were prepared from dehydrated potassium acetate intercalated through the guest-displacement reaction with ethylene glycol and glycerol. These materials were characterized and their behavior upon heating was investigated using X-ray diffraction, diffuse reflectance Fourier transform infrared spectroscopy, and combined thermogravimetry and differential scanning calorimetry coupled with mass spectroscopy. An intense perturbation of the AlAlOH stretching vibrations of kaolinite in the range 3700–3600 cm⁻¹ was observed for both of the intercalates, indicating strong interactions with the kaolinite surface OH groups. The two intercalates showed different thermal behavior. The ethylene glycol intercalates decomposed in a nitrogen atmosphere at 160 °C, with the release of the ethylene glycol from adjacent kaolinite layers. The glycerol intercalate showed a three-step decomposition over the temperature range 115–465 °C associated with dehydroxylation reactions, and a further decomposition reaction at 486 °C. The final reaction was due to the decomposition of the glycerol molecules grafted on the kaolinite surface and could be followed by monitoring the ion current in the mass spectrometer for masses corresponding to H₂O⁺, C₂H₄O⁺ and/or CO₂⁺, and O⁺ and/or CH₄⁺ molecular fragments, typical of the decomposition products of oxygen-bearing organic matter. Combined thermogravimetry-mass spectrometry proved to be an extremely useful tool for studying the thermal behavior of inorganic-organic layered hybrid materials.

Introduction

Kaolin is a common raw material in the ceramic industry and finds application as a filler in paper, plastics, paints, and rubber.^{1–4} The main mineral component of kaolin is kaolinite, a 1:1 clay mineral composed of single layers with a SiO₄ tetrahedral network connected to Al(O,OH)₆ octahedral networks, with platy particles of hexagonal and/or pseudo-hexagonal symmetry.⁵ The layers are held together via hydrogen bonds, dipolar interactions, and attractive Van der Waals forces, which result in a low intrinsic inner surface reactivity. Well ordered specimens differ little in composition from the ideal structural formula, Si₂Al₂O₅(OH)₄. However, it has been reported that octahedral iron may be present in poorly ordered kaolinites.^{6–8} Natural kaolinites have varying degrees of structural disorder, often related to their genesis conditions.^{9,10}

These structural variations may account for the different behavior of natural samples in the well-known intercalation reactions of kaolinites with dimethyl sulfoxide (DMSO) and urea.¹¹

Novel applications of kaolinite as a low cost precursor for hybrid systems, for example adsorbents and chromatographic materials, require its chemical modification.^{12–14} The preparation of these novel inorganic-organic systems requires intercalation of suitable guest molecules between the single kaolinite layers, after which new multilayer composites can be prepared by the guest-displacement method.¹⁵ Typical guest molecules for direct intercalation into kaolinite include

* To whom the correspondence should be addressed. E-mail: Marian.Janek@fns.uniba.sk; phone: +421 2 60296244; fax: +421 2 65429064.

[†] Comenius University.

[‡] Slovak Academy of Sciences.

[§] Research Centre Karlsruhe GmbH.

^{||} University Karlsruhe.

^{||} Our friend and colleague Prof. Dr. Rolf Nüesch passed away Dec 26, 2006.

- (1) Jepson, W. B. *Phil. Trans. R. Soc. London*, **1984**, A311, 411.
- (2) Bundy, W. M.; Ishley, J. N. *Appl. Clay Sci.* **1991**, 5, 397.
- (3) Bundy, W. M. In *Kaolin genesis and utilization, Special Publication No. 1*; Murray, H.; Bundy, W.; Harvey, C., Eds.; The Clay Minerals Society: Boulder, CO, 1993, p. 325.
- (4) Zbik, M.; Smart, R. St. C. *Clays Clay Miner.* **1998**, 46, 153.
- (5) Newman, A. C. D.; Brown, G. In *Chemistry of clays and clay minerals. Mineralogical Society Monograph No. 6*; Newman, A. C. D., Ed.; Longman Scientific & Technical: London, 1987; p 1.

- (6) Mestdagh, M. M.; Vielvoye, L.; Herbillon, A. J. *Clay Miner.* **1980**, 15, 1.
- (7) Petit, S.; Decarreau, A. *Clay Miner.* **1990**, 25, 181.
- (8) Brindley, G. W.; Kao, C. C.; Harrison, J. L.; Lipsicas, M.; Raythatha, R. *Clays Clay Miner.* **1986**, 34, 239.
- (9) Giese, R. F. In *Hydrous Phyllosilicates, Reviews in Mineralogy 19*; Bailey, S. W., Ed.; Mineralogical Society of America: Washington D.C., 1988; p 29.
- (10) Madejová, J.; Kraus, I.; Tunega, D.; Šamajová, E. *Geol. Carpathica, Ser. Clays* **1997**, 6, 3.
- (11) Lagaly, G. In *Tonminerale und Tone, Struktur, Eigenschaften, Anwendungen und Einsatz in Industrie und Umwelt*; Jasmund, K., Lagaly, G., Eds.; Steinkopff Verlag: Darmstadt, 1993; p 130.
- (12) Tunney, J. J.; Detellier, C. *Chem. Mater.* **1993**, 5, 747.
- (13) Tunney, J. J.; Detellier, C. *Clays Clay Miner.* **1994**, 42, 552.
- (14) Komori, Y.; Enoto, H.; Takenawa, R.; Hayashi, S.; Sugahara Y.; Kuroda, K. *Langmuir* **2000**, 16, 5506.
- (15) Weiss, A.; Thielepape, W.; Göring, G.; Ritter, W.; Schäfer, H. In *Proc. Int. Clay Conf., Stockholm*; Rosenqvist, Th., and Graff-Petersen, P., Eds.; Pergamon Press: Oxford, 1963; p 287.

potassium acetate,^{16–19} hydrazine,^{20,21} formamide,²² phenylphosphonic acid,²³ and the aforementioned dimethyl sulfoxide and urea.¹¹

A common feature of all of these substances is their ability to form and/or participate in strong hydrogen bonding or dipolar interactions, enabling intercalates of these molecules to be used in the guest-displacement reaction to form new supramolecular hybrid systems with substances which are not able to intercalate directly between the single kaolinite layers. Kaolinite intercalation has a disaggregating effect on the stacks of the layers, allowing the preparation of supramolecular structures of inorganic-organic layered materials to be used for, among other things, the calculation of the mineral's specific surface area,^{24,25} preparation of kaolinite-nanoparticle composites,^{26–30} or polymer-based nanohybrid materials.^{31,32}

Reports on intercalates of pyridine derivatives,³³ nitroanilines,^{34,35} amines,^{36,37} β -alanine,³⁸ polyethylene glycol,³⁹ and ethyl pyridinium chloride⁴⁰ prepared *via* guest-displacement reactions can be found in the literature. However, the practical application of such intercalates is rather limited because of their tendency to participate in subsequent guest-displacement reactions due to the weak attractive forces between the guest species and kaolinite layers. Much effort has therefore been focused on the possibility of involving the aluminol functional groups of kaolinite into the grafting reaction, to produce Al–O–C bonds, using alcohols such as methanol, ethylene glycol, ethanolamine, or polyols.^{12–14,41–44}

In a similar fashion to the studies using DMSO, an *N*-methylformamide-intercalated kaolinite has been used as the starting intercalate for guest-displacement reactions with alcohols, which were then characterized by X-ray diffraction (XRD), ¹³C nuclear magnetic resonance (NMR), Fourier transform infrared spectroscopy (FTIR), and thermogravimetry with differential scanning calorimetry (TG/DSC). Despite the application of such sophisticated analytical methods, Tunney and Detellier¹³ reported that there was no definite evidence for the formation of Al–O–C linkage; however, possible grafting on kaolinite layers could be expected. Furthermore, there are many reports in the literature of successfully grafted organic derivatives on related layered inorganic host materials, such as boehmite,^{46,47} layered double hydroxides,⁴⁸ and brucite.⁴⁹

The assumed model for the grafting reaction predicts that heating promotes production of surface bonded ethers, accompanied by the elimination of water molecules. Hence, excess water would hinder the reaction. Recently, Gardolinsky and Lagaly^{50,51} have shown that alcohol molecules grafted onto the kaolinite allow the incorporation of excess quantities of amines. The application of ultrasound to these heterointercalates in an organic solvent resulted in kaolinite delamination and the formation of “halloysite-like” nanotubes.

In the present study, we have tested the possibility of producing intercalates of ethylene glycol (EG) and glycerol (GL) using the guest-displacement reaction with dehydrated potassium acetate (KAc) intercalated kaolinite. The thermal behavior and grafting reaction was monitored using combined thermogravimetry and differential scanning calorimetry with mass spectroscopy of the gases evolved during heating. The use of mass spectroscopy offered a better understanding of intercalates' thermal behavior and the condensation reactions associated with the grafting of the alcohols onto the kaolinite layers. Subsequently, it was expected that possible simultaneous decomposition reactions of the intercalated molecules could be detected by this technique.

Experimental Section

Materials. A German kaolin from a primary deposit in Bayern-Oberpfalz was used in this study.⁵² The sample was washed with deionized Milli-Q water (18.2 M Ω ·cm⁻¹), dried at 65 °C, and crushed in an agate mortar. X-ray diffraction (XRD) and infrared (IR) analyses of this sample, hereafter referred to as KBO, confirmed that highly crystalline kaolinite was the only mineral phase present. Thermogravimetric analysis (20 mg sample, heating

- (16) Kristóf, J.; Mink, J.; Horváth, E.; Gábor, M. *Vib. Spectrosc.* **1993**, *5*, 61.
 (17) Maxwell, Ch. B.; Malla, P. B. U.S. Pat. No. 5672555, 1997.
 (18) Maxwell, Ch. B.; Malla, P. B. *Am. Ceram. Soc. Bull.* **1999**, *78*, 57.
 (19) Frost, R. L.; Kristóf, J.; Schmidt, J. M.; Klopogge, J. T. *Spectrochim. Acta A* **2001**, *57*, 603.
 (20) Barrios, J.; Plançon, A.; Cruz, M. I.; Tchoubar, C. *Clays Clay Miner.* **1977**, *25*, 422.
 (21) Martens, W. N.; Ding, Z.; Frost, R. L.; Kristóf, J.; Klopogge, J. T. *J. Raman Spectrosc.* **2001**, *33*, 31.
 (22) Kristóf, J.; Frost, R. L.; Klopogge, J. T.; Horváth, E.; Gábor, M. *J. Thermal Anal. Calor.* **1999**, *56*, 885.
 (23) Breen, C.; D'Mello, N.; Yarwood, J. *J. Mater. Chem.* **2002**, *12*, 273.
 (24) Dékány, I.; Szántó, F.; Rudzinski, W. *Acta Chim. Hung.* **1983**, *114*, 283.
 (25) Dékány, I.; Szántó, F.; Nagy, L. G. *J. Colloid Interf. Sci.* **1985**, *103*, 321.
 (26) Papp, Sz.; Dékány, I. *Prog. Colloid Polym. Sci.* **2001**, *117*, 94.
 (27) Patakfalvi, R.; Papp, Sz.; Dékány, I. In *Adsorption and Aggregation of Surfactants in Solutions*; Mittal, K. L., Shah, O., Eds.; Marcel Dekker Inc.: New York, 2003; p 269.
 (28) Patakfalvi, R.; Oszkó, A.; Dékány, I. *Colloid Surf. A* **2003**, *220*, 45.
 (29) Papp, Sz.; Patakfalvi, R.; Dékány, I. *Prog. Colloid Polym. Sci.* **2004**, *125*, 88.
 (30) Patakfalvi, R.; Dékány, I. *Appl. Clay Sci.* **2004**, *25*, 149.
 (31) Komori, Y.; Sugahara, Y.; Kuroda, K. *Chem. Mater.* **1999**, *11*, 3.
 (32) Elbokl, T. A.; Detellier, C. *J. Phys. Chem. Solids* **2006**, *67*, 950.
 (33) Sugahara, Y.; Satokawa, S.; Yoshioka, K.-I.; Kuroda, K.; Kato, C. *Clays Clay Miner.* **1989**, *37*, 143.
 (34) Kuroda, K.; Hiraguri, K.; Komori, Y.; Sugahara, Y.; Mouri, H.; Uesu, Y. *Chem. Commun.* **1999**, *22*, 2253.
 (35) Takenawa, R.; Komori, Y.; Hayashi, S.; Kawamata, J.; Kuroda, K. *Chem. Mater.* **2001**, *13*, 3741.
 (36) Komori, Y.; Sugahara, Y.; Kuroda, K. *J. Mater. Res.* **1998**, *13*, 930.
 (37) Komori, Y.; Sugahara, Y.; Kuroda, K. *Appl. Clay Sci.* **1999**, *15*, 241.
 (38) Itagaki, T.; Komori, Y.; Sugahara, Y.; Kuroda, K. *J. Mater. Chem.* **2001**, *11*, 3291.
 (39) Tunney, J. J.; Detellier, C. *Chem. Mater.* **1996**, *8*, 927.
 (40) Letaief, S.; Detellier, C. *J. Mater. Chem.* **2005**, *15*, 4734.
 (41) Tunney, J. J.; Detellier, C. *Clays Clay Miner.* **1994**, *42*, 473.
 (42) Tunney, J. J.; Detellier, C. *J. Mater. Chem.* **1996**, *6*, 1679.
 (43) Tunney, J. J.; Detellier, C. *Can. J. Chem.* **1997**, *75*, 1766.

- (44) Brandt, K. B.; Elbokl, T. A.; Detellier, C. *J. Mater. Chem.* **2003**, *13*, 2566.
 (45) Inoue, M.; Kondo, Y.; Inui, T. *Inorg. Chem.* **1988**, *27*, 215.
 (46) Inoue, M.; Tanino, H.; Kondo, Y.; Inui, T. *Clays Clay Miner.* **1991**, *39*, 151.
 (47) Inoue, M.; Kominami, H.; Kondo, Y.; Inui, T. *Chem. Mater.* **1997**, *9*, 1614.
 (48) Guimarães, J. L.; Marangoni, R.; Ramos, L. P.; Wypych, F. J. *Colloid Interf. Sci.* **2000**, *227*, 445.
 (49) Wypych, F.; Schreiner, W. H.; Marangoni, R. *J. Colloid Interf. Sci.* **2002**, *253*, 180.
 (50) Gardolinsky, J. E. F. C.; Lagaly, G. *Clay Miner.* **2005**, *40*, 537.
 (51) Gardolinsky, J. E. F. C.; Lagaly, G. *Clay Miner.* **2005**, *40*, 547.
 (52) Haus, R. In *Schriftenreihe für Angewandte Geowissenschaften 4*; Stör, M., Ed.; Verlag der Gesellschaft für Geowissenschaften e.V.: Berlin, 2002; p 19.

rate $10\text{ }^{\circ}\text{C}\cdot\text{min}^{-1}$) of KBO showed the highest dehydroxylation gradient at $550\text{ }^{\circ}\text{C}$ with a mass loss of 12.8%. This agrees closely with the mass loss of 13.9% predicted from the ideal structural formula of kaolinite $\text{Si}_2\text{Al}_2\text{O}_5(\text{OH})_4$. The observed dehydroxylation maximum, based upon the chosen experimental conditions, confirmed the XRD and IR data in indicating a highly crystalline kaolinite.⁵³ Environmental scanning electron microscopy of the KBO powder revealed aggregates of platy particles with lateral lengths of about $2.0\text{ }\mu\text{m}$ and typical hexagonal and/or pseudo-hexagonal symmetry. The aspect ratio (lateral length/height) of the KBO particles was estimated to be about 5.

The intercalates of ethylene glycol (EG, anhydrous, Merck, Germany) and glycerol (GL, anhydrous, Fluka, Germany) were prepared according to the guest-displacement method proposed by Weiss et al.¹⁵ The starting material, potassium acetate (KAc, p.a., Merck, Germany)-intercalated KBO, was prepared according to the method of Maxwell and Malla.^{17,18} Using kaolinite, KAc, and water mass fractions equal to 0.63, 0.26, and 0.11, respectively, these authors obtained more than 95% KAc intercalation. The potassium acetate intercalated KBO (KBO–KAc–water) was then dried in a Schlenk flask at $140\text{ }^{\circ}\text{C}$ and pressure $\leq 1\text{ mbar}$ for 4 days (KBO–KAc). The dried KBO–KAc intercalate was then dispersed in water-free ethylene glycol and glycerol in a glove box ($< 10\text{ ppm H}_2\text{O}$), with a final concentration of the KBO–KAc in dispersion of 25%. The samples were held at either room temperature or $65\text{ }^{\circ}\text{C}$ for up to 21 days, in tightly closed Nalgene flasks. The progress of the guest-displacement reactions was checked by XRD. Once the position of first basal reflection of intercalated kaolinite did not change, the samples KBO–EG or KBO–GL were washed four times with water-free ethylene glycol or glycerol respectively (solid concentration 25%) in a glove box. The efficiency of KAc removal was checked by ionic chromatography. Finally, the samples were washed three times in acetone or acetone/ethanol to remove KAc and excess of EG and GL, with an effectiveness greater than 98%. Finally, the samples were dried at $65\text{ }^{\circ}\text{C}$ in a drying oven for 24 h and crushed in an agate mortar.

One portion of each intercalate was characterized directly, and another was, based upon the initial TG analyses, heated at $200\text{ }^{\circ}\text{C}$ (KBO–EG) and $220\text{ }^{\circ}\text{C}$ (KBO–GL) for 2 h. The heating and cooling rate was $5\text{ }^{\circ}\text{C}\cdot\text{min}^{-1}$. The heated samples were characterized in the same manner as the nonheated intercalated materials.

Techniques. X-ray diffraction patterns from KBO intercalates were obtained using a Siemens D5000 diffractometer with Bragg–Brentano goniometer (Cu $\text{K}\alpha_1$ radiation $\lambda = 1.5405\text{ nm}$) equipped with a graphite secondary-beam monochromator. To prevent moisture adsorption from the air, the dried intercalates were transferred to a specially designed sample holder in a glove box and covered with Mylar foil. The patterns were recorded at room temperature, over the range $3\text{--}15^{\circ} 2\theta$, with a 0.02° step-size, and at least 1.5 s/step. The positions of the basal reflections were determined using the Bruker evaluation program *DiffraCplus*.

Infrared spectra of the KBO intercalates were measured by diffuse reflectance spectroscopy (DRIFTS unit from Spectratech) on a Bruker IFS 66/s Fourier transform infrared spectrometer equipped with a DTGS detector. Spectra were recorded over the range $4000\text{--}400\text{ cm}^{-1}$, accumulating 32 spectral scans, with a resolution of 4 cm^{-1} . Analysis by DRIFTS was preferred over a conventional pressed discs technique to avoid any unpredictable effects of pressure on the interlayer chemistry and reactions of the intercalates during disc preparation. To achieve a reasonable signal intensity and to avoid problems with specular reflectance,⁵⁴ the KBO

Table 1. Conditions of the STA Measurement

DSC/TG/MS	
sample amount	20 mg
grain size	powder
packing density	loosely packed, no pressing
reference material	empty crucible with lid
furnace atmosphere	50 mL/min air + 20 mL/min N_2 or 50 mL/min N_2 + 20 mL/min N_2
crucibles	Pt with lid or Al with lid
thermocouples	Pt/Pt ₉₀ Rh ₁₀
heating rate	$10\text{ }^{\circ}\text{C}/\text{min}$
temperature range	$35\text{--}550\text{ }^{\circ}\text{C}$ (Al crucible) $35\text{--}900\text{ }^{\circ}\text{C}$ (Pt crucible)

Table 2. Molecular Species Detected by MS Analysis

molecular mass, $\text{g}\cdot\text{mol}^{-1}$	corresponding summary formula
15	CH_3^+
16	O^+ and/or CH_4^+
18	H_2O^+
26	C_2H_2^+
28	CO and/or C_2H_4^+
32	CH_3OH^+
44	CO_2^+ and/or $\text{C}_2\text{H}_4\text{O}^+$
58	$\text{C}_3\text{H}_6\text{O}^+$
60	$\text{C}_2\text{H}_4\text{O}_2^+$
62	$\text{C}_2\text{H}_6\text{O}_2^+$

intercalates were diluted with dried potassium bromide (KBr) powder with a mass ratio of 1:100 (a ratio which had been optimized during preliminary investigations), and about 200 mg of the powder mixture was then analyzed. The background was collected prior to sample analysis using an aluminum mirror. The DRIFT spectra were converted to the absorbance equivalent data using the Kubelka–Munk algorithm.

A Simultaneous Thermal Analysis (STA) device STA 449C (Netzsch Gerätebau GmbH, Germany) with a TG/DSC sample holder linked to a Quadrupole Mass Spectrometer QMS 403C (InProcess Instruments/Netzsch Gerätebau GmbH, Germany) allowed simultaneous collection of signals due to mass loss, heat flow, and evolved gases during heating and was used for monitoring of intercalate reactivity. The conditions for the STA measurement can be found in Table 1.

About 20 mg of KBO intercalate was weighed into an aluminum or platinum crucible and placed in the STA, which was purged either with air or nitrogen. The low sample weight was necessary because of the sensitivity of the instrument toward the decomposition of organic matter. The list of ionic masses detected by MS, and their corresponding molecular species, can be found in Table 2. Platinum crucibles were used for the analysis of the kaolinite and KAc intercalate at higher temperatures. The KBO–KAc intercalate was heated to a maximum temperature of $900\text{ }^{\circ}\text{C}$, while the KBO–GL and KBO–EG intercalates were heated to a maximum temperature of only $550\text{ }^{\circ}\text{C}$. The reason for this was to minimize the risk of condensation of organic decomposition products on the transit capillaries connecting the TG with the MS, which could only be heated to a maximum temperature of $250\text{ }^{\circ}\text{C}$. Changes in buoyancy and the specific heat capacity of the sample holder and the crucibles were corrected by analyzing empty crucibles under the same experimental conditions as used for the sample measurements. Data interpretation was performed using the Netzsch Proteus Thermal Analysis software package.

Results and Discussion

Characteristics of the Kaolinite Intercalates. The changes in the position of the first basal reflection of the KBO upon KAc–water intercalation and its subsequent drying at

(53) Smykatz-Kloss, W. In *Differential Thermal Analysis*; Springer-Verlag: Heidelberg, 1974; p 66.

(54) Madejová, J.; Komadel, P. *Clays Clay Miner.* **2001**, *49*, 410.

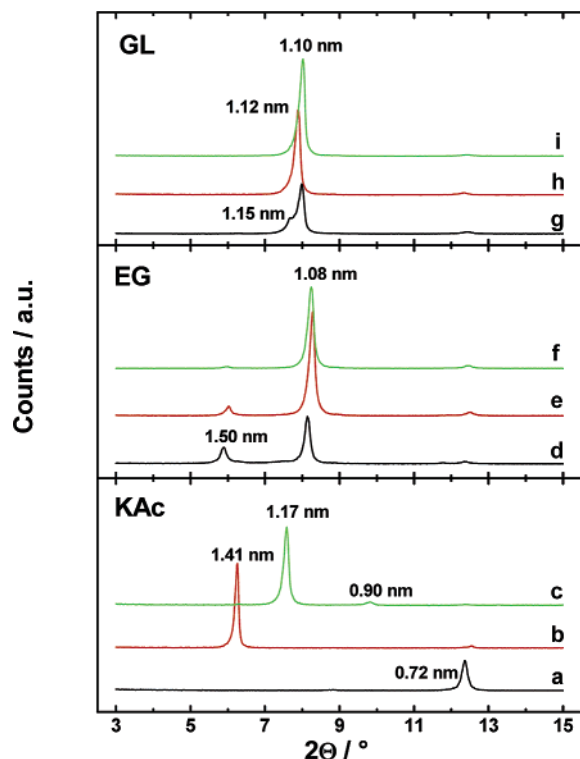


Figure 1. Changes in the position of the first basal reflection, determined by X-ray diffraction for KAc intercalates: (a) starting KBO kaolinite, (b) KBO–KAc–water intercalate, (c) KBO–KAc intercalate; guest-displacement with EG (d) after 3 days, (e) after 10 days, (f) after 19 days of reaction at room temperature; guest-displacement with GL (g) after 1 day, (h) after 10 days, (i) after 21 days of reaction at 65 °C.

140 °C for 4 days (≤ 1 mbar pressure) are shown in Figure 1. The d -spacing of 0.72 nm for the starting kaolinite increased to 1.41 nm upon intercalation of KAc and water molecules into the structure (Figure 1), an expansion which is typical for KAc–water intercalated kaolinites.^{16,18} The low-intensity peak at 0.71 nm corresponds to the second basal reflection of the KBO–KAc–water intercalate. The amount of water used for intercalation would lead to formation of a two-layer potassium hydrate, with a corresponding interlayer expansion of about 0.46 nm. However, the presence of the acetate anion results in the observed 0.69 nm expansion.⁵⁵

The diffraction pattern shown in Figure 1 indicates that approximate 100% intercalation of KBO with KAc–water had been achieved. The removal of water molecules from the interlayer cavity by the application of heat under vacuum resulted in a decrease of the first basal spacing to 1.17 nm. The weak reflection at 0.90 nm is possibly due to either the small excess of dried KAc in the sample or the presence of a KOH intercalate. Such an intercalate could be formed upon removal of a small amount of acetate in the form of acetic acid from the interlayer.

Changes in the XRD patterns during the guest-displacement reaction of KBO–KAc with EG at room temperature are shown in the Figure 1. Penetration of EG into the interlayer space of kaolinite leads to the KAc molecules being solvated with EG, as demonstrated by the reflection at 1.50 nm after reaction for 3 days with dried KBO–KAc, a

reflection with even higher d -spacing than that found for the water-hydrated KAc intercalate. The most intense reflection in the diffraction pattern, which increased in intensity over time, was observed at 1.08 nm, corresponding to the KBO–EG intercalate. The exchange of KAc with EG was effective, with over 95% of the KBO–EG intercalate being formed after 19 days. A small amount of the kaolinite was observed to deintercalate to its original form, indicated by the reflection at 0.72 nm.

The effect of temperature upon the rate of guest-displacement reaction was subsequently investigated, by repeating the experiment at 65 °C (data not shown). At the higher temperature, the extent of the guest-displacement reaction with EG was similar after 12 h to that observed at room temperature after 10 days.

On the basis of these results, and the much higher viscosity of GL compared to EG, the guest-displacement reaction with GL was performed only at 65 °C (Table 3). Figure 1 shows the changes in the XRD patterns during guest-displacement reaction with GL. After 1 day, two peaks were visible, at 1.15 and 1.10 nm, due to the dried KBO–KAc intercalate and the KBO–GL intercalate, respectively. Comparing this pattern with that obtained from the EG guest-displacement reaction, a slightly different mechanism is evident. Clearly, the KAc molecules were not highly solvated, as was observed for EG intercalation. However, the replacement of KAc with GL molecules in the interlayer space still occurred. After reaction for 10 days, only one asymmetric peak, at 1.12 nm, was observed. Longer reaction times led to a slight reduction in the first basal spacing, to 1.10 nm, after 21 days, indicating the intercalation of GL molecules between the kaolinite layers, and displacement of the residual KAc. Similarly, as was observed in the case of EG, a small amount of kaolinite deintercalated, leading to a reflection at 0.72 nm.

To verify the existence and nature of the intercalated molecules, DRIFT spectra of the various intercalates were measured. Figure 2 compares the DRIFT spectra of the starting KBO kaolinite with the KBO–KAc intercalate prior to, and after, drying at 140 °C. The spectrum of the KBO starting material was typical for a well-ordered kaolinite. Well-resolved Al–OH stretching and bending bands were observed at 3700–3600 cm^{-1} and 950–900 cm^{-1} , respectively. Stretching vibrations typical of the SiO groups present in 1:1 layered silicates were seen in the 1110–1000 cm^{-1} region, while the bending vibrations were observed in the range 790–690 cm^{-1} . A more detailed description of the absorption bands of the starting materials and intercalated substances are summarized in Table 4.^{48,54}

The intercalation of KAc and water molecules into the KBO resulted in the weakening of the hydrogen bonds between adjacent kaolinite layers. The negatively charged oxygen atoms on the acetate ions were involved in hydrogen bonds with inner surface hydroxyl groups. Consequently a band at 3605 cm^{-1} was observed in the spectrum (Figure 2b). Considering the intensity of this band, and the marked decrease in the intensity of the bands at 3668 and 3653 cm^{-1} , a significant number of inner surface OH groups must have been interacting with solvated KAc. The band at 3605 cm^{-1} overlapped that of the vibrations of inner hydroxyls, observed

(55) Güven, N. In *CMS Workshop Lectures, Vol. 4, Clay-water interface and its rheological implications*; Güven, N., Pollastro, R. M., Eds.; The Clay Minerals Society: Boulder, CO, 1992; p 2.

Table 3. Selected Physical and Chemical Properties of the Compounds Used for Intercalation⁵⁶

Substance	Structural formula	M_r g·mol ⁻¹	ρ^a g·cm ⁻³	η^b mPa·s	m.p. / b.p. / a.i. ^c °C
Potassium Acetate	H ₃ C-COOK	98.1	1.57	-	292 / - / -
Ethylene Glycol		62.1	1.11	16.1 / 3.3	-13 / 197 / 398
Glycerol		92.1	1.26	934 / 39.8	18 / 290 / 370

^a Density at 20 °C. ^b Viscosity at 25/75 °C. ^c Melting point/boiling point/autoignition temperature.

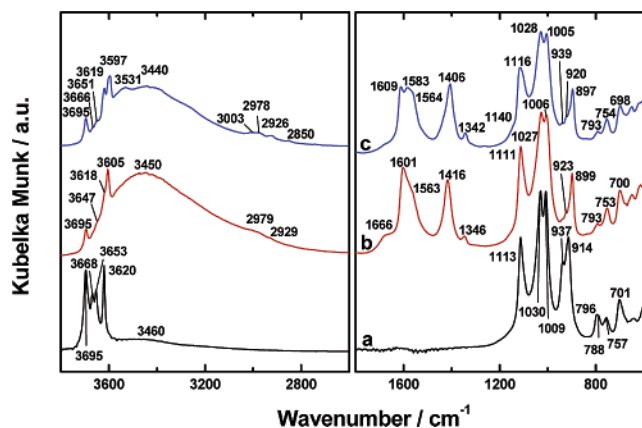


Figure 2. DRIFT spectra of (a) starting KBO kaolinite, (b) KBO-KAc-water intercalate, (c) KBO-KAc intercalate.

as a shoulder, at 3618 cm⁻¹, which indicate a fraction of OH groups not to have been affected by H-bonding with solvated KAc. The position of the band at 3695 cm⁻¹, attributed to the outer OH groups of kaolinite, did not change in frequency, but the intensity of this band was reduced significantly due to the presence of KAc. The broad band with a maximum at 3450 cm⁻¹ was attributed to stretching vibrations of water and indicates the presence of water, along with KAc molecules, between adjacent elementary layers of kaolinite. The weak shoulders, at 2979 and 2929 cm⁻¹, were attributed to CH₃ stretching vibrations of acetate (Figure 2b).

The intercalation of KAc and water also strongly affected the AlAlOH bending bands at 937 and 914 cm⁻¹. The SiO stretching vibrations in the 1110–1000 cm⁻¹ region, and the bending vibrations in the range of 790–690 cm⁻¹, were considerably less affected by the presence of the new chemical species intercalated between the kaolinite layers. The band corresponding to the bending vibrations of the inner surface OH groups, observed at 937 cm⁻¹ disappeared, and only one sharp band, at 899 cm⁻¹, was seen in Figure 2b. Clearly, the perturbation of the vibrations of the structural OH groups is a sensitive indicator of the environment of these functional groups. The changes in the AlAlOH bending bands at 938 and 920 cm⁻¹ suggest the distortion of both inner surface and inner OH groups upon KAc intercalation. A broad band near 1660 cm⁻¹ was attributed to the bending vibration of water molecules at high salt concentrations.⁵⁷ The intense bands at 1601 and 1416 cm⁻¹ correspond to

$\nu_{as}(\text{COO}^-)$ and $\nu_s(\text{COO}^-)$ stretching vibrations, respectively, of an aliphatic acid salt (Table 4).

Removal of water molecules from the KBO-KAc-water intercalate by drying resulted in a significant decrease in intensity of the broad band at 3450 cm⁻¹. Nevertheless, the intensity remained such that a relatively high amount of water was retained in this sample. However, the STA analyses indicated that the easily removable water content in this sample was less than 0.4%. The AlAlOH stretching vibrations in the range of 3700–3600 cm⁻¹ indicated a change in the environment of the OH groups upon partial water removal (Figure 2c). Some of the inner surface OH groups were present in environments similar to those found in raw kaolinite, as indicated by the bands at 3666, 3651, and 3619 cm⁻¹. The OH stretching band at 3597 cm⁻¹ reflects strong hydrogen bonding of the inner surface OH groups with KAc upon removal of solvating water molecules of KAc. The previously weak shoulders at 2979 and 2929 cm⁻¹, seen in the spectrum of the hydrated KBO-KAc intercalate and attributed to CH₃ stretching vibrations of the acetate anion, were more clearly resolved, together with additional bands, at 3003 and 2850 cm⁻¹.

Upon water removal, a weak shoulder in the SiO stretching region, located at 1140 cm⁻¹, could be observed. The OH bending region showed the same downward shift in the AlAlOH band, to 899 cm⁻¹, and two weaker bands, at 939 and 920 cm⁻¹, were detected. The change in vibrational frequencies of the inner OH groups support the assumption that potassium cations located in the ditrigonal cavity of the tetrahedral sheets can interact even with inner OH groups. Splitting of the $\nu_{as}(\text{COO}^-)$ band into the doublet at 1609 and 1583 cm⁻¹ indicated a change in the character of the H-bonded inner surface hydroxyls. Finally, the $\nu_s(\text{COO}^-)$ band of KAc at 1416 cm⁻¹ underwent a small shift to 1406 cm⁻¹. These changes are in good agreement with the XRD analyses, indicating that intercalation of KAc between the adjacent layers of kaolinite significantly affects the spectral properties of the elementary sheets.

Figure 3 shows the DRIFT spectra of KBO-EG and KBO-GL intercalates after being washed with acetone and dried at 65 °C. Strong interactions of EG with the structure of kaolinite could be deduced from the spectral changes of

(56) *Handbook of chemistry and physics*; Lide, D. R., Ed.; CRC Press: Boca Raton, FL, 1998.

(57) Madejová, J.; Janek, M.; Komadel, P.; Herbert, H.-J.; Moog, H. C. *Appl. Clay Sci.* **2002**, *20*, 255.

Table 4. Attribution of FTIR Absorption Bands for the Kaolinite and Intercalates with Potassium Acetate, Ethylene Glycol, and Glycerol

wavenumber (cm ⁻¹)	attribution
3695	OH stretching of inner-surface hydroxyl groups 1 of kaolinite
3670	OH stretching of inner-surface hydroxyl groups 2 of kaolinite
3652	OH stretching of inner-surface hydroxyl groups 2 of kaolinite
3620	OH stretching of inner hydroxyl groups of kaolinite
3460	OH stretching of water
1630	OH deformation of water
3450–3250	OH stretching of EG/GL
2965	CH stretching (antisymmetric)
2940	CH stretching (symmetric)
2880	CH stretching
1600–1550	COO ⁻ stretching of aliphatic acid salt (antisymmetric)
1400–1300	COO ⁻ stretching of aliphatic acid salt (symmetric)
1460–1360	CH ₂ deformation
1250	COH stretching or CH ₂ deformation
1115	Si–O stretching (longitudinal mode)
1103	Si–O stretching (perpendicular)
1040–1005	Si–O stretching (in-plane)
938	OH deformation of inner-surface hydroxyl groups
920	OH deformation of inner hydroxyl groups
915–900	C–C stretching, gauche conformation
790	Si–O
755	Si–O (perpendicular)
695	Si–O (perpendicular)

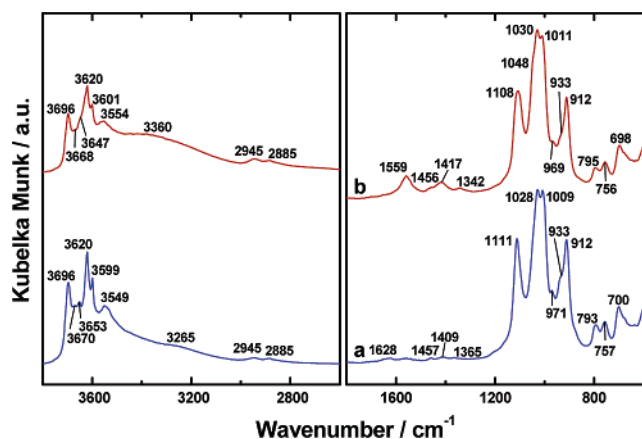


Figure 3. DRIFT spectra of (a) KBO–EG and (b) KBO–GL intercalates after being washed with acetone and dried at 65 °C.

the AlAlOH stretching and bending bands. The stretching bands observed at 3668 and 3653 cm⁻¹ (Figure 2a) merged into a single intense band at 3599 cm⁻¹ (Figure 3a), but some OH groups remained in their original environment (indicated by weak bands at 3670 and 3653 cm⁻¹). At the same time, bands were observed at 3696 and 3620 cm⁻¹, i.e. at the same frequencies as seen in the KBO and KBO–KAc samples. Additionally, we suppose that some of the inner surface OH groups were involved in the interaction with EG and contributed to the band at 3599 cm⁻¹.

The bands at 3549 and 3265 cm⁻¹ were due to OH stretching vibration of the EG. Typical stretching vibrations of CH₂ groups were present at 2945 and 2885 cm⁻¹ and bending bands at 1457, 1409, and 1365 cm⁻¹. The presence of a weak band at 1628 cm⁻¹ may have been attributed to the bending band of water, which had possibly been introduced during washing of the KBO–EG intercalates with acetone and after drying at 65 °C.

Intense interactions of GL with the kaolinite layers, in a similar fashion to the EG intercalate, were inferred from the changes of the AlAlOH stretching and bending bands (Figure 3b). A new band at 3601 cm⁻¹ appeared (Figure 3b) together with a weak shoulder at 3647 cm⁻¹ and a band at 3668 cm⁻¹.

Additionally, unaffected bands were observed at 3696 and 3620 cm⁻¹. Stretching vibrations of the OH groups of the GL molecules could be seen as broad bands at 3554 and 3360 cm⁻¹, while the CH₂ and CH groups could be seen at 2945 and 2885 cm⁻¹. The bending bands of the CH₂ and CH groups of the GL located between adjacent KBO layers were observed at 1456 and 1342 cm⁻¹. The band at 1556 cm⁻¹ may result from residual KAc. The AlAlOH bending region revealed the presence of a new, weaker band at 970 and shoulder at 933 cm⁻¹ for both EG and GL intercalates (Figure 3).

Thermal Behavior of the Intercalates. Typical thermoanalytical results of the decomposition, under nitrogen, of the KBO–KAc–water intercalate are shown in Figure 4, in the form of DSC–TG–MS curves. Heating of this intercalate up to a temperature of 140 °C resulted in a mass loss of 11%. As would be expected, the main evolved compound was water (H₂O⁺), indicated by the emission of an ion with molar mass 18 g·mol⁻¹ in the MS curve. This observed mass loss corresponded perfectly with the amount of water used for the preparation of the KBO–KAc–water intercalate.

The MS curve for M = 18 showed a main evolution peak at 109 °C, corresponding with the minimum on the DSC curve. Subsequently, a second peak appeared on the MS curve, at 117 °C. We therefore propose that two molecular water fractions were released upon heating. First, a lower temperature component (30–113 °C) corresponding to external surface water and some of the inner surface molecules hydrating KAc. Second, a higher temperature portion (~113–140 °C) corresponding to the remaining inner surface water hydrating KAc. At these temperatures, small quantities of species with a molar mass of 16 g·mol⁻¹ were detected in the corresponding MS curve. This species may be O⁺ and/or CH₄⁺, which are typically detected during the decomposition processes of oxygen bearing organic substances.

Further heating, up to 340 °C, revealed a small endothermic peak, with an onset temperature of 292 °C, attributed

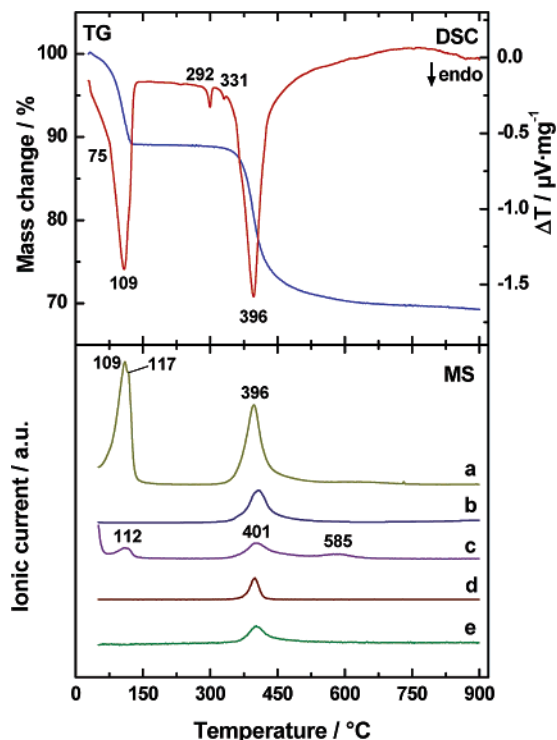


Figure 4. Thermal behavior of KBO–KAc–water intercalate as detected with DSC, TG, and MS (streaming N₂, Pt crucible). Ionic intensity curves are shown for species with (a) 18, (b) 44, (c) 16, (d) 58, (e) 26 g·mol⁻¹ (Table 2).

to melting of KAc (Table 3), and some rearrangement of the dehydrated KAc between the adjacent layers of KBO, detected through the presence of the second endothermic peak on the DSC curve at 331 °C. The main endothermic process, associated with dehydroxylation of kaolinite layers and decomposition of the acetate anion, occurred at 395 °C (according to the maximum in the mass change gradient), indicating that intercalation of the KAc decreased the dehydroxylation temperature of the kaolinite by about 155 °C. Acetate anion decomposition was observed via the simultaneous release of species with masses; 44 g·mol⁻¹ (C₂H₄O⁺ and/or CO₂⁺), 58 g·mol⁻¹ (C₃H₆O⁺), and 26 g·mol⁻¹ (C₂H₂⁺) together with 18 g·mol⁻¹ (H₂O⁺) and 16 g·mol⁻¹ (O⁺ and/or CH₄⁺) molecular fragments. Some evolution of ions of mass $M = 16$ was still detected at about 585 °C. The mass loss resulting from these simultaneous decomposition processes was 22.5%, comprising a 12.8% change for kaolinite dehydroxylation and 9.7% for cracking of the acetate anion. A simple mass balance indicates that about one-half of acetate must be retained by the kaolinite in the form of coke (Figure 4).

The thermal behavior of dried KBO–KAc intercalate (data not shown) was very similar to the KBO–KAc–water intercalate; however, the mass change to 140 °C was less than 0.4%. The MS data showed just a small amount of 18 g·mol⁻¹ and no 16 g·mol⁻¹ species up to this temperature. This confirmed a low water content in the KBO–KAc samples used for the guest-displacement reactions. The highest mass change gradient, associated with the dehydroxylation of kaolinite and the decomposition of acetate, was observed at 398 °C, a temperature similar to the nondried intercalate.

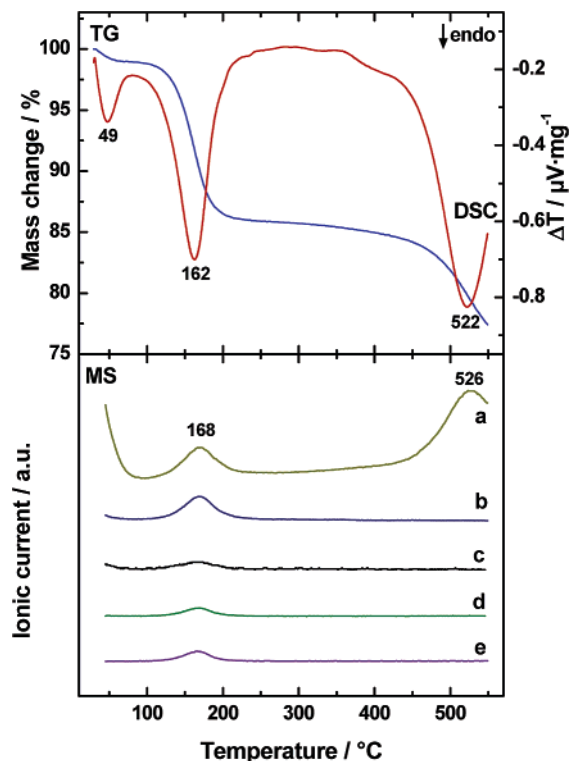


Figure 5. Thermal behavior of KBO–EG intercalate as detected with DSC, TG, and MS (streaming N₂, Al crucible). Ionic intensity curves are shown for species with (a) 18, (b) 44, (c) 16, (d) 26, (e) 62 g·mol⁻¹ (Table 2).

Combined TG-MS analysis may be used to follow the grafting process by examining the reactivity of the intercalated EG/GL molecules and detection of specific decomposition products arising from numerous simultaneous reactions. These reactions can be divided into three groups, as follows: (i) reactions corresponding to the grafting of alcohol with structural OH groups of kaolinite, resulting in the elimination of water as the main product; (ii) dehydration and decomposition reactions of alcohol upon interaction with the kaolinite surface, producing water, oxygen and molecular fragments containing carbon; (iii) decomposition reactions of grafted molecules on the kaolinite surface, detected via the identification of specific carbon-containing molecular fragments that are preferentially formed from the ether bonded organic molecules. In accordance with literature data, it is reasonable to expect that the latter group of reactions occur at higher temperatures than the former two.¹³

The effect of heating on the reactivity of the intercalated EG molecules was investigated using the KBO–EG intercalate, and the results are shown in Figure 5. This sample released about 1% of its mass as physically adsorbed water, up to temperature of 80 °C. This was indicated by the detection of 18 g·mol⁻¹ (H₂O⁺) molecular fragments, along with small amount of 16 g·mol⁻¹ (O⁺ and/or CH₄⁺), and 44 g·mol⁻¹ (CO₂⁺ and/or C₂H₄O⁺), species. At higher temperatures, there was an intense endothermic reaction accompanied by a mass loss of about 14%, with a highest mass change gradient at 160 °C. The molecular fragments detected by MS indicated that this reaction corresponded to the release of EG and its decomposition. Species with molar mass of 18 g·mol⁻¹ (H₂O⁺), 44 g·mol⁻¹ (CO₂⁺ and/or C₂H₄O⁺), 16 g·mol⁻¹ (O⁺ and/or CH₄⁺), and 26 g·mol⁻¹ (C₂H₂⁺) were

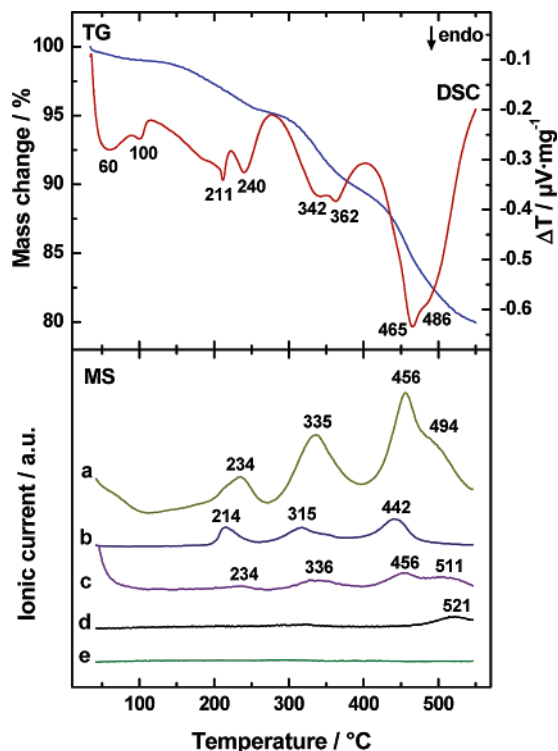


Figure 6. Thermal behavior of KBO-GL intercalate as detected with DSC, TG, and MS (streaming N_2 , Al crucible). Ionic intensity curves are shown for species with (a) 18, (b) 44, (c) 16, (d) 15, (e) 26 $g \cdot mol^{-1}$ (Table 2).

clearly detected at 168 °C along with a 62 $g \cdot mol^{-1}$ ($C_2H_6O_2^+$) fragment corresponding to the EG molecule.

There was a further endothermic reaction at 522 °C, corresponding to the dehydroxylation of kaolinite, with water being the only species detected by MS. Therefore, it may be assumed that decomposition of the KBO-EG was complete at temperatures below 200 °C. The EG started to decompose at temperatures lower than its boiling point (Table 3), probably also due to the catalytic effect of kaolinite layers.⁵⁸ In the experiment repeated in air, no exothermic reaction corresponding to the oxidation of EG molecules was detected, and it was possible that all of the EG molecules had been removed before the temperature was high enough to achieve oxidation. Despite the fact that the extent of all of the simultaneous reactions was difficult to estimate, no grafting of EG on the KBO layers was detected, because no species originating from EG molecules were detected at temperatures above 200 °C.

The KBO-GL intercalate showed a much more complicated thermal behavior than the KBO-EG intercalate, with several mass loss steps observed in the TG curve obtained under nitrogen (Figure 6). Physically adsorbed water was released at temperature up to 115 °C, with a mass loss of about 1% and two endothermic peaks, at 60 and 100 °C. This was followed by a mass loss of about 4% over the temperature range 115–260 °C and two endothermic peaks, at 211 and 240 °C. These reactions correspond to two dehydration and possible decomposition reaction of GL. The species detected by MS were typical and similar to those seen in the case of EG (18 $g \cdot mol^{-1}$ (H_2O^+), 44 $g \cdot mol^{-1}$

(CO_2^+ and/or $C_2H_4O^+$), and 16 $g \cdot mol^{-1}$ (O^+ and/or CH_4^+)). These molecular fragments were again detected over the temperature range of 260–370 °C, with two endothermic peaks, at 342 and 362 °C, and a mass loss of about 5%.

Over the range 370–550 °C there was a further mass loss of over 10%. This was associated with a broad endothermic peak, with a minimum at 465 °C and a clear shoulder at 486 °C. Interestingly, the temperature 465 °C correlated well with the evolution of the dehydration and decomposition products discussed above including species such as 18 $g \cdot mol^{-1}$ (H_2O^+), 44 $g \cdot mol^{-1}$ (CO_2^+ and/or $C_2H_4O^+$), and 16 $g \cdot mol^{-1}$ (O^+ and/or CH_4^+). Conversely, the temperature 486 °C corresponded to the evolution of species with 18 $g \cdot mol^{-1}$ (H_2O^+), 16 $g \cdot mol^{-1}$ (O^+ and/or CH_4^+), and 15 $g \cdot mol^{-1}$ (CH_3^+). No molecular fragments corresponding to 26 $g \cdot mol^{-1}$ ($C_2H_2^+$) or 58 $g \cdot mol^{-1}$ ($C_3H_6O^+$) were detected over the whole temperature window used in the experiment. These MS data indicate that in the course of heating KBO-GL intercalate, partial grafting of GL molecules on the KBO layers can be expected due to the detection of the decomposition products at 486 °C. The dehydroxylation of the structural OH groups of kaolinite not involved in the reaction with GL possibly starts at 465 °C. However, it is concurrent with the dehydration and decomposition of GL. The decomposition of KBO-GL intercalate under air was the same as under nitrogen (Figure 6), up to a temperature of 230 °C. However, there was an intense oxidation reaction over the temperature range 230–383 °C, with maximum heat flow at 305 °C (see also Table 3).

To investigate the effect of heating on the properties of the powdered EG and GL intercalates, on the basis of the TG analyses, the KBO-EG and KBO-GL samples were heated at 200 °C and 220 °C, respectively. The changes in the position of the first basal reflection of the KBO-EG upon washing the sample with acetone and heating at 200 °C for 2 h are shown in Figure 7. The figure shows clearly that removal of the excess EG with acetone had almost no effect on the prepared intercalate and basal distance of kaolinite layers. Conversely, upon heating there was a slight decrease in d -spacing, to 1.07 nm, with a marked decrease in intensity. Additionally, the reflection at 0.72 nm was more prominent after heating. The breadth of the diffraction peaks indicated the presence of disordered kaolinite layers in their parallel orientation. From the initial >95% of EG presented between adjacent elementary kaolinite layers, as was assessed from the comparison of the integral intensities of first basal reflections, less than 55% was retained upon heating at 200 °C for 2 h. This result agreed very well with the DSC-TG-MS results, confirming that EG is removed from the intercalate, resulting in a disordered kaolinite phase.

Figure 7 also shows the diffraction patterns of KBO-GL upon washing the sample with acetone/ethanol and 2 h heating at 220 °C. The removal of excess GL by washing slightly broadened the reflection at 1.10 nm, while heating the sample to 220 °C resulted in the shift of the basal reflection to 1.09 nm. From the initial >95% of GL presented between adjacent elementary kaolinite layers, about 94% remained after heating at 220 °C for 2 h. The KBO-GL intercalate was more thermally stable than the KBO-EG

(58) Occelli, M. L. In *Catalysis today: Pillared clays*; Burch, R., Ed.; 1988; Vol. 2; p 339.

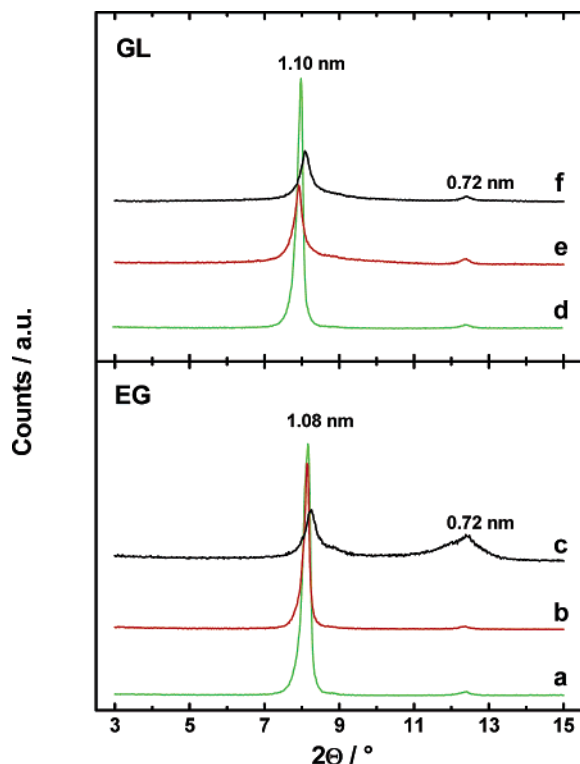


Figure 7. Changes in the position of the first basal reflection, determined by X-ray diffraction for KBO-EG intercalates: (a) KBO-EG intercalated kaolinite, (b) KBO-EG intercalate upon washing with acetone, (c) KBO-EG intercalate upon heating at 200 °C; and KBO-GL intercalates: (d) KBO-GL intercalated kaolinite, (e) KBO-GL intercalate upon washing with acetone/ethanol, (f) KBO-GL intercalate upon heating at 220 °C.

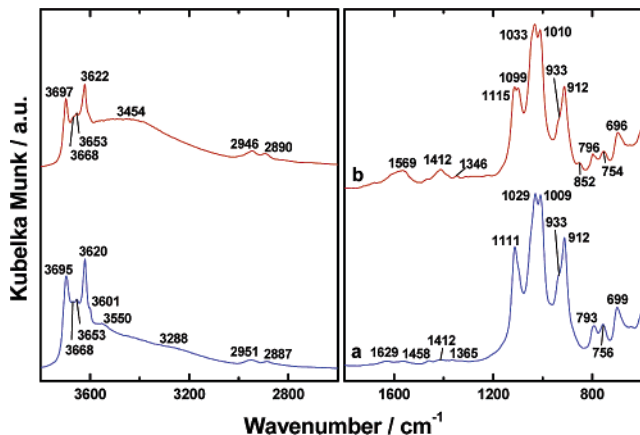


Figure 8. DRIFT spectra of (a) KBO-EG and (b) KBO-GL intercalates after being heated for 2 h at 200 and 220 °C, respectively.

intercalate, due to the higher boiling point of GL than EG (Table 3).

The DRIFT spectra of heated KBO-EG and KBO-GL are shown in Figure 8. Compared to the unheated samples (Figure 3) there was a clear decrease in the band intensities at 3600 cm^{-1} of both the EG and GL intercalates. At the same time, the Al-OH stretching vibrations in the range 3700–3600 cm^{-1} and Al-OH bending bands at 940–910 cm^{-1} showed a clear change in OH environment, toward a state similar to the starting raw kaolinite (Figure 2a). This was much more pronounced after heating the KBO-EG intercalate than the KBO-GL intercalate. The same could be postulated about the Si-O stretching bands at 1100–1000 cm^{-1} and the bending vibrations at 790–690 cm^{-1} of

KBO-EG. Interestingly, in the case of GL, the Si-O stretching vibration was a doublet, at 1115 and 1099 cm^{-1} , and a new band at 852 cm^{-1} appeared after heating to 220 °C. The band at 852 cm^{-1} could be attributed to the rocking vibration of CH_2 groups of GL, indicating that heating induced partial grafting into the kaolinite layers. Some GL molecules may have been present in the form of an alkene derivative upon its dehydration between the kaolinite layers, depending on the treatment temperature, as found from DSC-TG-MS experiments.

Despite clay minerals being well-known for their cracking catalytic reactivity,⁵⁷ and the fact that partial decomposition during the grafting of EG onto boehmite layers has already been reported by Inoue et al.,⁴⁵ the question arises as to why the EG decomposes without being grafted onto the KBO layers already at 160 °C. It is known that the formation of the 0.93 nm phase is hindered significantly if the water content in the reaction mixture with EG is above 2 volume % (~ 1.8 mass %).¹³ Additionally, a significant portion of nonmodified kaolinite, detected via a 0.71 nm *d*-spacing, was found in the reaction product based on the kaolinite-DMSO intercalate. In this study, we have achieved more than 95% intercalation using dehydrated KBO-KAc intercalate. Such a high intercalation efficiency was achieved with EG only under water-free conditions when using the kaolinite-DMSO intercalate.

The TG-MS measurements showed that the easily removable water content of the KBO-EG, released by heating to 80 °C, was only about 1 mass %. This water may have been outer surface moisture, possibly adsorbed upon ethanol washing of the respective intercalate. It cannot be excluded that some water was absorbed by the EG and retained as inner surface moisture, gradually hindering the grafting of EG upon release over the temperature range 80–226 °C. The decomposition products of EG were detected simultaneously over this temperature interval.

It may also be perceivable, that both EG and GL intercalates contained a small fraction of water molecules strongly hydrogen bonded with structural OH groups of kaolinite, giving rise to adsorption bands in the infrared spectra at about 3600 cm^{-1} . However, this type of absorption band has only been detected in samples prepared with about 5 volume % (~ 4.5 mass %) of water or in a water hydrate of kaolinite.^{13,41} Considering our great efforts to protect the dehydrated KBO-KAc intercalate from humidity, as seen by the relatively low intensities of the water stretching (3400–3200 cm^{-1}) and bending (1600 cm^{-1}) vibrations, an additional effect hindering EG grafting reaction should be considered.

It is possible that any traces of KAc present upon the guest-displacement reaction may impact upon the reactivity of EG with kaolinite aluminol groups. Many studies have reported data where the grafting reactions were performed with excess quantities of alcohol.^{12–14,41,42} This may indicate a mass action law, where excess EG molecules over the kaolinite aluminol surface is favorable for the grafting process. Finally, there are no accessible data comparing kaolinites of different origin, hence different chemical compositions or even polytypes, with regard to their intercalation behavior and

grafting reactions. The specific orientation of the hydroxyl groups of different kaolinites induced by variation in their chemical composition may affect the kaolinite behavior. It is known and documented in the literature that there is a variability in the ease with which kaolinites of different origin may be intercalated with dimethyl sulfoxide and urea.¹¹ Hence it is reasonable to suppose that a combination of all of the factors mentioned above plays a significant role in the grafting ability of EG and GL onto kaolinite when these are intercalated by KAc displacement.

Conclusions

This study has shown that ethylene glycol and glycerol intercalates of kaolinite can be prepared from dehydrated potassium acetate intercalate through guest-displacement reactions. Intercalates, stable under air and at room temperature, were achieved after removal of excess ethylene glycol or glycerol by washing with acetone or acetone/ethanol mixture. An intense perturbation of AlAlOH stretching vibrations of the kaolinite in the range 3700–3600 cm^{-1} was observed for the ethylene glycol and glycerol intercalates, indicating their strong interactions with the surface OH groups of kaolinite.

Different thermal behavior was observed for both intercalates. The ethylene glycol intercalate decomposed at 160 °C with the release of ethylene glycol located between the

adjacent layers of kaolinite. This process was easily monitored by mass spectrometer evolution curves and the detection of mass fragments corresponding to H_2O^+ , CO_2^+ and/or $\text{C}_2\text{H}_4\text{O}^+$, O^+ , and/or CH_4^+ , typical for the decomposition products of oxygen bearing organic matter. The kaolinite layers dehydroxylated at 522 °C upon removal of ethylene glycol. The glycerol intercalate meanwhile showed a three-step dehydroxylation decomposition in the temperature range 115–465 °C and a further decomposition step at 486 °C, corresponding to the decomposition of the glycerol molecules grafted on the kaolinite surface. Clearly, the grafting efficiency was decreased due to the simultaneous decomposition of intercalated glycerol molecules; hence, a technique to quantify the fraction of OH groups that effectively reacted to Al–O–C bonds and to characterize the products of grafting reaction must be developed.

Acknowledgment. The authors acknowledge financial support as a part of FZK research project No. 5270.0046.0012 and of Slovak Grant Agency VEGA 1/4457/07. The kind assistance of Ms. D. Rapp (ITC-WGT, FZK) during the TG-MS measurements is greatly appreciated. M. Janek thanks Dr. J. Madejová for critical review of IR data of an earlier version of the manuscript and to Dr. L. Black who helped improve the language and style of the final version of the manuscript.

CM061481+